Mg^{2+} Modulates Voltage-dependent Activation in Ether-à-go-go Potassium Channels by Binding between Transmembrane Segments S2 and S3

William R. Silverman, Chih-Yung Tang, Allan F. Mock, Kyung-Bong Huh, and Diane M. Papazian

From the Department of Physiology and Molecular Biology Institute, University of California Los Angeles School of Medicine, Los Angeles, California 90095-1751

ABSTRACT Extracellular Mg^{2+} directly modulates voltage-dependent activation in ether-à-go-go (eag) potassium channels, slowing the kinetics of ionic and gating currents (Tang, C.-Y., F. Bezanilla, and D.M. Papazian. 2000. *J. Gen. Physiol.* 115:319-337). To exert its effect, Mg^{2+} presumably binds to a site in or near the eag voltage sensor. We have tested the hypothesis that acidic residues unique to eag family members, located in transmembrane segments S2 and S3, contribute to the Mg^{2+}-binding site. Two eag-specific acidic residues and three acidic residues found in the S2 and S3 segments of all voltage-dependent K^+ channels were individually mutated in *Drosophila* eag, mutant channels were expressed in *Xenopus* oocytes, and the effect of Mg^{2+} on ionic current kinetics was measured using a two electrode voltage clamp. Neutralization of eag-specific residues D278 in S2 and D327 in S3 eliminated Mg^{2+}-sensitivity and mimicked the slowing of activation kinetics caused by Mg^{2+} binding to the wild-type channel. These results suggest that Mg^{2+} modulates activation kinetics in wild-type eag by screening the negatively charged side chains of D278 and D327. Therefore, these residues are likely to coordinate the bound ion. In contrast, neutralization of the widely conserved residues D284 in S2 and D319 in S3 preserved the fast kinetics seen in wild-type eag in the absence of Mg^{2+}, indicating that D284 and D319 do not mediate the slowing of activation caused by Mg^{2+} binding. Mutations at D284 affected the eag gating pathway, shifting the voltage dependence of Mg^{2+}-sensitive, rate limiting transitions in the hyperpolarized direction. Another widely conserved residue, D274 in S2, is not required for Mg^{2+} sensitivity but is in the vicinity of the binding site. We conclude that Mg^{2+} binds in a water-filled pocket between S2 and S3 and thereby modulates voltage-dependent gating. The identification of this site constrains the packing of transmembrane segments in the voltage sensor of K^+ channels, and suggests a molecular mechanism by which extracellular cations modulate eag activation kinetics.

KEY WORDS: voltage clamp • structural model • kinetics • voltage sensor • metal binding site

INTRODUCTION

The *Drosophila ether-à-go-go* (eag) gene and its homologues encode a distinct subfamily of voltage-gated K^+ channels (Warmke et al., 1991; Brüggemann et al., 1993; Warmke and Ganetzky, 1994; Wei et al., 1996). In most members of the eag family, activation kinetics are dramatically regulated by extracellular Mg^{2+}, an effect that is not seen in other types of voltage-gated K^+ channels (Terlau et al., 1996; Frings et al., 1998; Schönherr et al., 1999; Tang et al., 2000). Analysis of eag ionic and gating currents indicates that Mg^{2+} directly modulates the process of voltage-dependent gating, presumably by binding to a site in or near the voltage sensor (Terlau et al., 1996, Tang et al., 2000). To investigate the mechanism by which Mg^{2+} regulates voltage-dependent activation and to gain novel insights into the structure and function of the voltage sensor, we have identified the Mg^{2+}-binding site in eag channels.

In proteins, bound Mg^{2+} ions are often coordinated by the acidic side chains of aspartate and glutamate residues (da Silva and Williams, 1991). Therefore, our analysis focused on acidic amino acids found in and near transmembrane segments S2 through S4, a region that includes essential components of the voltage sensor in K^+ channels (Liman et al., 1991; Papazian et al., 1991, 1995; Perozo et al., 1994; Planells-Cases et al., 1995; Aggarwal and MacKinnon, 1996; Mannuzzu et al., 1996; Seoh et al., 1996; Cha and Bezanilla, 1997; Cha et al., 1999; Glauner et al., 1999). Segments S2 and S3 contain three acidic residues that are conserved among all subfamilies of voltage-gated K^+ channels (Warmke and Ganetzky, 1994; Chandy and Gutman, 1995). Previous work indicates that these residues make important contributions to the biogenesis, structure, and function of the voltage sensor in Shaker K^+ channels (Papazian et al., 1995; Planells-Cases et al., 1995;

C.-Y. Tang's current address is Department of Neurology, UCLA School of Medicine, Los Angeles, CA 90095.

Address correspondenceto Diane M. Papazian, Ph.D., Department of Physiology, UCLA School of Medicine, Los Angeles, CA 90095-1751. Fax: (310) 206-5661; E-mail: papazian@mednet.ucla.edu

Seoh et al., 1996; Tiwari-Woodruff et al., 1997, 2000). In the *Drosophila* eag channel, these residues correspond to D274 and D284 in S2 and D319 in S3 (see Fig. 1 A). In addition to these highly conserved positions, segments S2 and S3 contain two acidic amino acids, D278 in S2 and D327 in S3, that are conserved only among members of the eag subfamily (see Fig. 1 B) (Warmke and Ganetzky, 1994; Chandy and Gutman, 1995). Because these residues are restricted to the eag family, they are prime candidates to contribute to the Mg^{2+}-binding site.

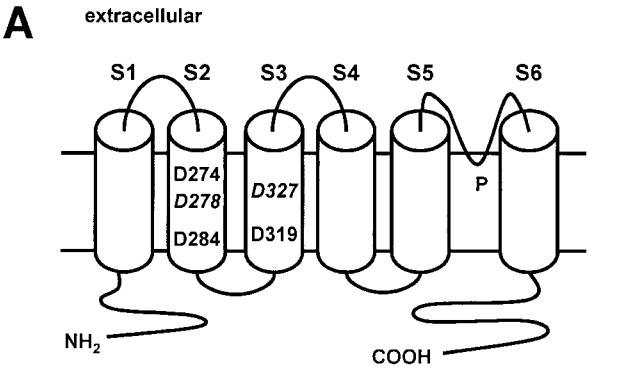

B

	S2			S3	
	274	278	284	319	327
	↓	↓	↓	↓	↓
d eag	VV	DSIV	DVIFFI	DIVLNFH	FIIDLLSCLPYDVFNAF
r eag1	VV	DSIV	DVIFLV	DIVLNFH	FVIDLLSCLPYDVINAF
b eag1	VV	DSIV	DVIFLV	DIVLNFH	FVIDLLSCLPYDVINAF
r erg3	VV	DLIV	DIMFII	DILINFR	FLIDMVAAIPFDLLIFG
h erg	VV	DLIV	DIMFIV	DILINFR	FLIDMVAAIPFDLLIFG
d erg	VV	DSIV	DVIFFI	DIVLNFH	FLIDLVAAVPFDLLLVG
d elk	VS	DVIV	EALFIV	DILLNFR	FALDLLAALPFDHLYAS
d ShB	LI	ETLC	IIWFSF	ELVVRFF	NVIDIIAIIPYFITLAT
r Kv2.1	HV	EAVC	IAWFTM	EYLLRFL	NAIDLLAILPYYVTIFL
r Kv3.1	YI	EGVC	VVWFTF	EFLMRVV	NAIDFVAIIPFYLEVGL
m Kv4.1	CM	DTAC	VLIFTG	EYLLRLF	SLIDVVAILPYYIGLFV

FIGURE 1. Acidic amino acids within the voltage sensor of eag. (A) A model is shown for the membrane topology of the *Drosophila* eag K^+ channel subunit containing six transmembrane segments (S1–S6) and the P-region. The approximate locations of acidic amino acids within the second and third transmembrane segments are indicated. Italics denote eag-specific acidic residues. (B) Sequence alignment of S2 and S3 segments from voltage-dependent K^+ channels, with acidic residues shown in bold. Segments S2 and S3 can be aligned unambiguously due to the presence of highly conserved residues, including three acidic residues (Chandy and Gutman, 1995). Members of the eag subfamily differ from other voltage-dependent K^+ channels due to the presence of additional acidic amino acids in S2 and S3 (Warmke and Ganetzky, 1994). Sequences shown are from eag family members and representative members of Kv1-Kv4 families (Chandy and Gutman, 1995; Shi et al., 1997; Ganetzky et al., 1999). Arrows indicate acidic residues that were mutated in this study. Numbering corresponds to the *Drosophila* eag sequence. Abbreviations used are: d, *Drosophila*; r, rat; b, bovine; h, human; m, mouse; erg, eag related gene; elk, eag-like K^+ channel gene; Sh, Shaker.

The mechanism of voltage-dependent activation has been extensively studied in K^+ channels, notably Shaker channels (Bezanilla et al., 1994; Hoshi et al., 1994; Zagotta et al., 1994b; Larsson et al., 1996; Mannuzzu et al., 1996; Schoppa and Sigworth, 1998a,b; Smith-Maxwell et al., 1998; Cha et al., 1999; Glauner et al., 1999; Ledwell and Aldrich, 1999). Membrane depolarization initiates a series of voltage-dependent conformational changes that increase the probability of pore opening. Entry into the open state involves a less voltage-dependent and highly cooperative transition (Hoshi et al., 1994; Zagotta et al., 1994a,b; Ledwell and Aldrich, 1999). A conserved negatively charged residue in S2 and several positively charged residues in S4 contribute to the protein's ability to detect and respond to changes in membrane potential (Aggarwal and MacKinnon, 1996; Seoh et al., 1996). During activation, the S4 residues traverse much or all of the transmembrane electric field (Aggarwal and MacKinnon, 1996; Larsson et al., 1996; Seoh et al., 1996; Starace et al., 1997; Baker et al., 1998). Fluorescent measurements suggest that the S2 segment is involved in conformational changes that precede S4 movement during gating (Cha and Bezanilla, 1997).

The voltage sensor is contained in a domain of the channel that includes S2 through S4 at a minimum, with a possible structural contribution from segment S1 (Papazian et al., 1995; Tiwari-Woodruff et al., 1997; Hong and Miller, 2000; Li-Smerin et al., 2000a,b). Evidence for tertiary structural interactions between charged residues in S2, S3, and S4 has been obtained using second site suppressor analysis (Papazian et al., 1995; Tiwari-Woodruff et al., 1997). At least some of these interactions are state dependent, occurring in a subset of the conformations along the activation pathway, consistent with the dynamic role of the voltage sensor in channel gating (Tiwari-Woodruff et al., 2000).

Voltage-dependent activation in eag can be described reasonably well by a sequential model in which each subunit undergoes two voltage-dependent transitions that prime the channel for opening, followed by a cooperative and less voltage-dependent step that opens the pore (Tang et al., 2000). One notable feature of eag activation is that voltage-dependent transitions that occur at more hyperpolarized potentials are rate limiting for pore opening, which is not true in Shaker channels (Bezanilla et al., 1994; Zagotta et al., 1994b; Terlau et al., 1996; Schönherr et al., 1999; Tang et al., 2000). Analysis of eag ionic and gating currents suggests that extracellular Mg^{2+} modulates rate limiting transitions that occur at hyperpolarized potentials, and voltage-dependent transitions close to the open state (Tang et al., 2000). In the activation model, the effects of Mg^{2+} can be simulated by reducing the forward and backward rates of the first voltage-dependent transition, and

to a lesser extent, the forward rate of the second voltage-dependent transition (Tang et al., 2000).

To test the hypothesis that eag-specific acidic residues in S2 and S3 contribute to the Mg^{2+}-binding site, these residues and others were individually mutated to determine the effect on sensitivity to Mg^{2+}. The results indicate that Mg^{2+} binds between segments S2 and S3, and thereby modulates activation gating in eag channels.

MATERIALS AND METHODS

Molecular Biology

Mutations in eag were generated by PCR using a three or four primer strategy (Landt et al., 1990; Sarkar and Sommer, 1990). PCR products were digested with appropriate restriction enzymes and transferred into a pGEMHE subclone of wild-type eag (Tang and Papazian, 1997). Transferred regions containing mutations were verified by dideoxy sequencing.

Constructs were linearized with NotI before in vitro transcription using the mMessage mMachine kit (Ambion). RNA encoding wild-type and mutated eag channels was injected into *Xenopus* oocytes for electrophysiological analysis (Timpe et al., 1988; Tang and Papazian, 1997).

Electrophysiology

Ionic currents from wild-type and mutant eag channels were recorded at room temperature (20–22°C) using a two electrode voltage clamp as described previously (Timpe et al., 1988; Papazian et al., 1991). Oocytes were bathed in normal Ringer's solution, containing 118 mM NaCl, 1.8 mM $CaCl_2$, 10 mM HEPES, pH 7.2. The bath solution also contained from 0 to 20 mM $MgCl_2$, as indicated. To record eag tail currents, KCl was substituted for an equal concentration of NaCl, as noted. Electrodes contained 3 M KCl and had resistances of 0.3–1.0 MΩ.

Voltage pulse protocols were applied and data were acquired using pClamp v5.5.1 software and a TL-1 Labmaster interface (Axon Instruments, Inc.). The sampling rate was varied as needed to resolve activation kinetics. Data were filtered at 0.2 to 2 kHz using an 8-pole Bessel filter (Frequency Devices), and digitized at a frequency five times higher than the filter frequency. Linear capacitive and leak currents were subtracted using a P/−4 protocol (Bezanilla and Armstrong, 1977).

Activation kinetics were compared in the absence and presence of $MgCl_2$, using concentrations up to 20 mM. Ionic currents were evoked by pulsing from a holding potential of −80 or −90 mV to voltages ranging from −60 mV to +60 or +100 mV in 20 mV increments. Activation kinetics were quantified in two ways as previously described (Tang et al., 2000). The late rising phase of the ionic current was fitted with a single exponential component to derive a time constant for activation, τ. Alternatively, the time to half maximal current amplitude was measured to obtain a value for $t_{1/2}$. These methods gave compatible results. Values of τ and $t_{1/2}$ are provided as mean ± SEM.

The probability of opening as a function of voltage was determined by measuring the amplitude of isochronal tail currents in 89 mM KCl bath solution. Ionic currents were evoked by pulsing from a holding potential of −90 mV to voltages ranging from −70 mV to +80 mV in 10 mV increments. Tail currents were recorded upon return to −90 mV. Tail current amplitudes were determined at isochronal points ranging from 4 to 10 ms following repolarization, normalized to the maximum value, and plotted versus test potential. The data were fitted with a single Boltzmann equation using Origin 5.0 software (Microcal) to obtain a slope factor and midpoint potential.

The effect of prepulse hyperpolarization on activation kinetics was investigated in the presence and absence of Mg^{2+} (Cole and Moore, 1960). From a holding potential of −90 mV, wild-type channels were subjected to 50 ms prepulses to voltages ranging from −150 mV to −50 mV in 10 mV increments, followed by a test pulse to +60 mV. For mutant channels, the prepulse duration was increased to 250 ms and the range was extended in the depolarized direction, as noted.

RESULTS

Modulation of Activation Kinetics by Mg^{2+}

The *Drosophila* eag K^+ channel was expressed in *Xenopus* oocytes. Ionic currents were recorded using a two electrode voltage clamp in the presence and absence of 10 mM extracellular Mg^{2+}, a concentration that produced a near maximal slowing of activation kinetics (see Fig. 4 B). Eag kinetics were quantified in two ways (Tang et al., 2000). A single exponential component was fitted to the late phase of activation to estimate a time constant (τ) for the process (Fig. 2 A). However, this τ value does not adequately describe the initial time course of the ionic current, which displays sigmoid kinetics (Ludwig et al., 1994; Terlau et al., 1996; Tang et al., 2000). Therefore, the time to half maximal current amplitude ($t_{1/2}$) was also measured (Fig. 2 B) (Tang et al., 2000). The $t_{1/2}$ value reflects changes in both the delay and time course of the ionic current.

Mg^{2+} slowed eag kinetics throughout the activation voltage range, with a larger effect after smaller depolarizations (Fig. 2) (Tang et al., 2000). Mg^{2+} decelerated activation by ~10-fold at 0 mV, compared with 4-fold at +100 mV. To investigate whether eag activation kinetics become Mg^{2+}-independent at very depolarized voltages, plots of τ and $t_{1/2}$ versus test potential were extrapolated beyond the experimentally accessible voltage range. Both plots were well fitted by single exponential functions (Fig. 2), which were used to predict limit values for τ and $t_{1/2}$ at infinite positive voltage. This procedure resulted in estimates of 6 ms for τ_{lim} in the presence of Mg^{2+}, compared with ~2 ms in its absence. Similarly, $t_{1/2lim}$ was estimated to be 12 ms in the presence and ~4 ms in the absence of Mg^{2+}. Thus, Mg^{2+} is predicted to slow activation kinetics by about threefold at infinite positive voltage.

As previously described, hyperpolarizing prepulses also decelerate eag activation, increasing the delay and decreasing the rate of onset of ionic currents evoked by a subsequent test pulse (Ludwig et al., 1994; Terlau et al., 1996; Schönherr et al., 1999; Tang et al., 2000). In combination with hyperpolarizing prepulses, 10 mM Mg^{2+} produced a longer delay before the onset of ionic currents and further slowed activation kinetics (Fig. 3 A). These effects were quantified by measuring τ and $t_{1/2}$ as a function of prepulse potential in the presence and absence of Mg^{2+} (Fig. 3 B). The data reveal the existence of rate-limiting, Mg^{2+}-sensitive transitions that

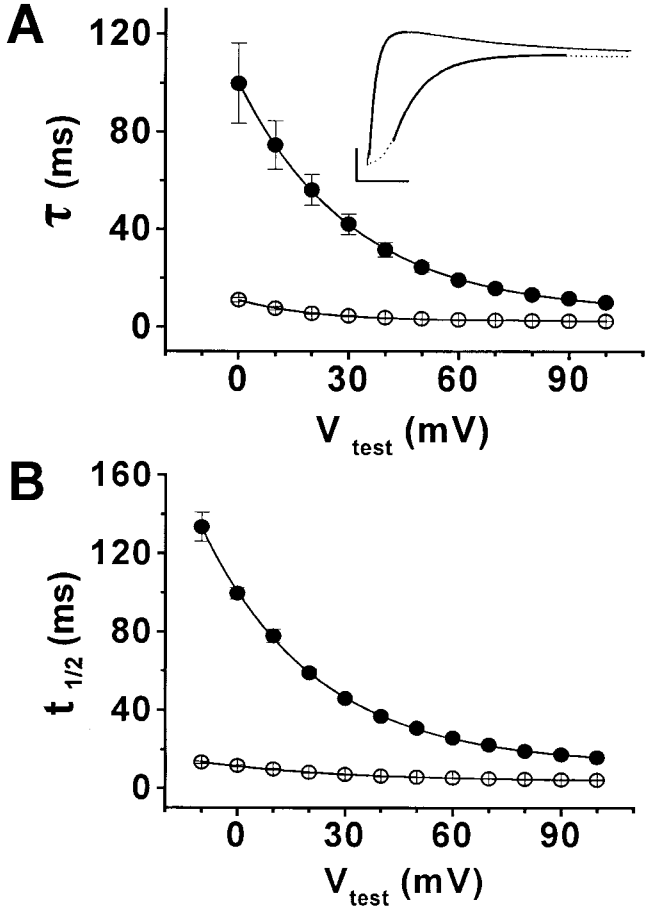

FIGURE 2. Mg^{2+} slows activation of wild-type eag. (A) Activation time constants (τ) obtained in the presence (●) or absence (○) of 10 mM Mg^{2+} have been plotted versus test pulse potential. Currents were evoked by depolarizing from a holding potential of −90 mV to the indicated voltages. A single exponential component was fitted to the late rising phase of ionic currents to derive τ values. Data are shown as mean ± SEM, $n = 5$. In this and subsequent figures, if error bars are not visible, the SEM was smaller than the size of the symbols. At 0 mV, $\tau = 100 \pm 16.4$ ms in the presence of 10 mM Mg^{2+}, and 11.1 ± 0.9 ms in the absence of Mg^{2+}. At +100 mV, $\tau = 10.0 \pm 0.7$ ms in the presence of 10 mM Mg^{2+}, and 2.3 ± 0.06 ms in the absence of Mg^{2+}. The data were fitted with single exponential functions (solid curves) to estimate values for τ_{lim} at infinite positive voltage (see text). (Inset) Fits with single exponential functions (bold curves) are shown superimposed on current traces evoked by depolarizing to +60 mV in the presence (dashed line) or absence (solid line) of 10 mM Mg^{2+}. Bars: 2 μA and 25 ms. (B) The time to half maximal current amplitude ($t_{1/2}$) at +60 mV was measured in the presence (●) or absence (○) of 10 mM Mg^{2+} and plotted versus test potential. Values are shown as mean ± SEM, $n = 5$. At 0 mV, $t_{1/2} = 100 \pm 3.0$ ms in the presence of 10 mM Mg^{2+}, and 11.6 ± 0.6 ms in the absence of Mg^{2+}. At +100 mV, $t_{1/2} = 15.8 \pm 0.5$ ms in the presence of 10 mM Mg^{2+}, and 4.3 ± 0.2 ms in the absence of Mg^{2+}. The data were fitted with single exponential functions (solid curves) to estimate values for $t_{1/2lim}$ at infinite positive voltage (see text).

occur at hyperpolarized potentials during the activation of wild-type eag channels (Tang et al., 2000).

D278 Mutations Eliminate Mg^{2+} Sensitivity

Eag-specific acidic residues in S2 and S3 are good candidates to bind Mg^{2+} because of their location in the voltage sensing domain and their conservation in the eag subfamily. Neutralization of D278, the eag-specific acidic residue in S2, in the mutant D278V eliminated Mg^{2+} modulation of activation kinetics (Fig. 4). Fig. 4 A (left) shows currents evoked by depolarizing from −80 mV to +60 mV in the presence and absence of 10 mM Mg^{2+}. Whereas wild-type eag showed measurable changes in activation kinetics upon exposure to 1 mM Mg^{2+}, D278V was insensitive to Mg^{2+} concentrations as high as 20 mM (Fig. 4 B). Ionic current kinetics in D278V were unaffected by extracellular Mg^{2+} throughout the voltage range for activation (data not shown).

Interestingly, the conservative mutation D278E also had Mg^{2+}-insensitive activation kinetics (Fig. 4 A, right, and B). This is significant because the glutamate substitution in D278E retains a carboxylic acid side chain, but is longer by one methylene group than the original aspartate residue. These data suggest that the mutation prevents Mg^{2+} from binding because the binding site is sterically constrained in the vicinity of D278.

Activation kinetics in D278V and D278E were quantified as a function of prepulse potential (Fig. 4 C). In these mutants, rate-limiting transitions were accessed at hyperpolarized potentials, as indicated by an increase in τ after hyperpolarizing prepulses (Fig. 4 C, left). Values for $t_{1/2}$ showed a similar trend (Fig. 4 C, right). Extracellular Mg^{2+} did not modulate the kinetics of these transitions, however (Fig. 4 C). An extended range of prepulses was used for D278V because this mutation shifted the probability of opening versus voltage (Po–V) curve in the depolarized direction compared with wild-type eag and the mutant D278E (Fig. 4 D). The transition to slower activation kinetics occurred at more depolarized potentials in D278V than in wild-type or D278E channels (Fig. 4 C).

Significantly, the D278V and D278E mutations had differential effects on eag activation kinetics. Although both mutants were insensitive to extracellular Mg^{2+}, the activation kinetics of D278E, which retains a negatively charged side chain, were rapid, resembling those of the wild-type channel in the absence of Mg^{2+} (Fig. 4, A and C). In contrast, the kinetics of D278V were slow, similar to those of the wild-type channel in the pres-

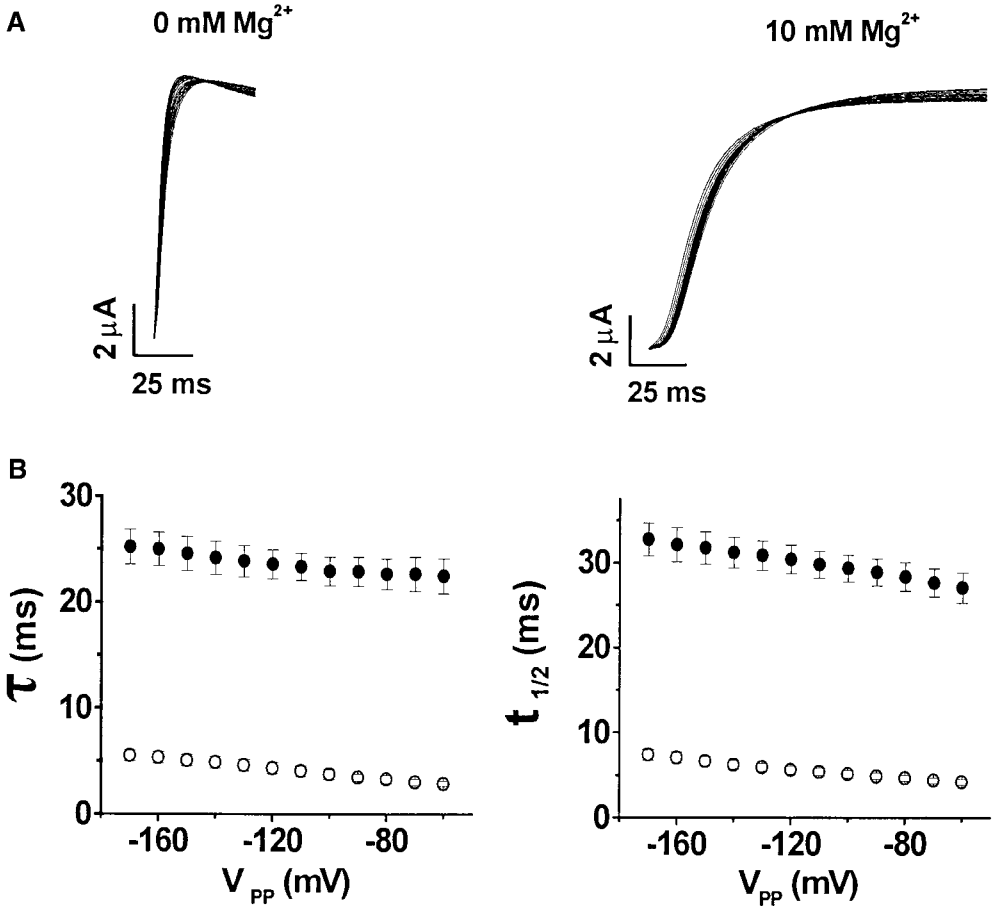

FIGURE 3. Hyperpolarizing prepulses decelerate activation in wild-type eag. (A) From a holding potential of −90 mV, 50 ms prepulses to voltages ranging from −170 to −60 mV were applied in 10 mV increments, followed by a test pulse to +60 mV. Representative currents evoked in the absence (left) or presence (right) of 10 mM Mg^{2+} are shown. (B, left) Values of τ were obtained from single exponential fits to the late rising phase of currents evoked at +60 mV in the presence (●) or absence (○) of 10 mM Mg^{2+} and plotted versus prepulse potential. Data are shown as mean ± SEM, n = 5. (B, right) Values of $t_{1/2}$ at +60 mV were measured in the presence (●) or absence (○) of 10 mM Mg^{2+} and plotted versus prepulse potential. Values are shown as mean ± SEM, n = 5.

ence of Mg^{2+} (Fig. 4, A and C). These results suggest that Mg^{2+} slows activation kinetics in wild-type eag in part by screening the negative charge at position D278. The neutralization mutation D278V mimics the Mg^{2+}-bound state of wild-type eag, in which the charge at D278 is shielded by the ion, whereas D278E resembles the Mg^{2+}-free state of wild-type eag, in which the charge is unshielded. These data support the conclusion that D278 in S2 contributes to the binding site by coordinating the Mg^{2+} ion.

D327 Mutations Dramatically Reduce Mg^{2+} Sensitivity

D327, the eag-specific acidic residue in S3, was replaced by alanine or phenylalanine to generate the mutants D327A and D327F. Phenylalanine is found in the analogous position in Shaker channels (Fig. 1 B).

Extracellular Mg^{2+} concentrations up to 20 mM had no significant effect on activation kinetics in D327A channels (Fig. 5, A and B). In this mutant, the late phase of activation was not well fitted by a single exponential component (data not shown), so activation kinetics were estimated by measuring $t_{1/2}$ (Fig. 5 C, right). Mg^{2+} had no significant effect on $t_{1/2}$ over the tested prepulse range (Fig. 5 C), which was extended to −40 mV because D327A shifted the Po–V curve in the depolarized direction (Fig. 5 D).

In contrast, Mg^{2+} slightly slowed the kinetics of D327F channels (Fig. 5 C). Values of τ and $t_{1/2}$ were determined as a function of prepulse potential in the presence and absence of Mg^{2+} (Fig. 5 C). In D327F, the value of $t_{1/2}$ increased from ~33 ms in the absence of Mg^{2+} to ~53 ms in the presence of 20 mM Mg^{2+}, a difference that is statistically significant ($P < 0.05$, ANOVA) (Fig. 5 B). A small residual sensitivity to Mg^{2+} was also apparent when τ was plotted as a function of prepulse potential (Fig. 5 C). One interpretation of these results is that the negatively charged τ electrons associated with the phenyl ring in phenylalanine may be able to interact weakly with Mg^{2+} in D327F (Dougherty 1996; Williams et al., 1998; Wouters, 1998).

D327F and D327A channels exhibited slow activation kinetics whether Mg^{2+} was present or absent (Fig. 5 A). In D327F, values for τ and $t_{1/2}$ resembled those of wild-type eag measured in the presence of Mg^{2+}, whereas $t_{1/2}$ values in D327A were even longer (Fig. 5 C). Thus, neutralization of D327 resulted in activation kinetics that were qualitatively similar to those of the Mg^{2+}-bound state of wild-type eag. These data suggest that Mg^{2+} slows activation kinetics in the wild-type channel in part

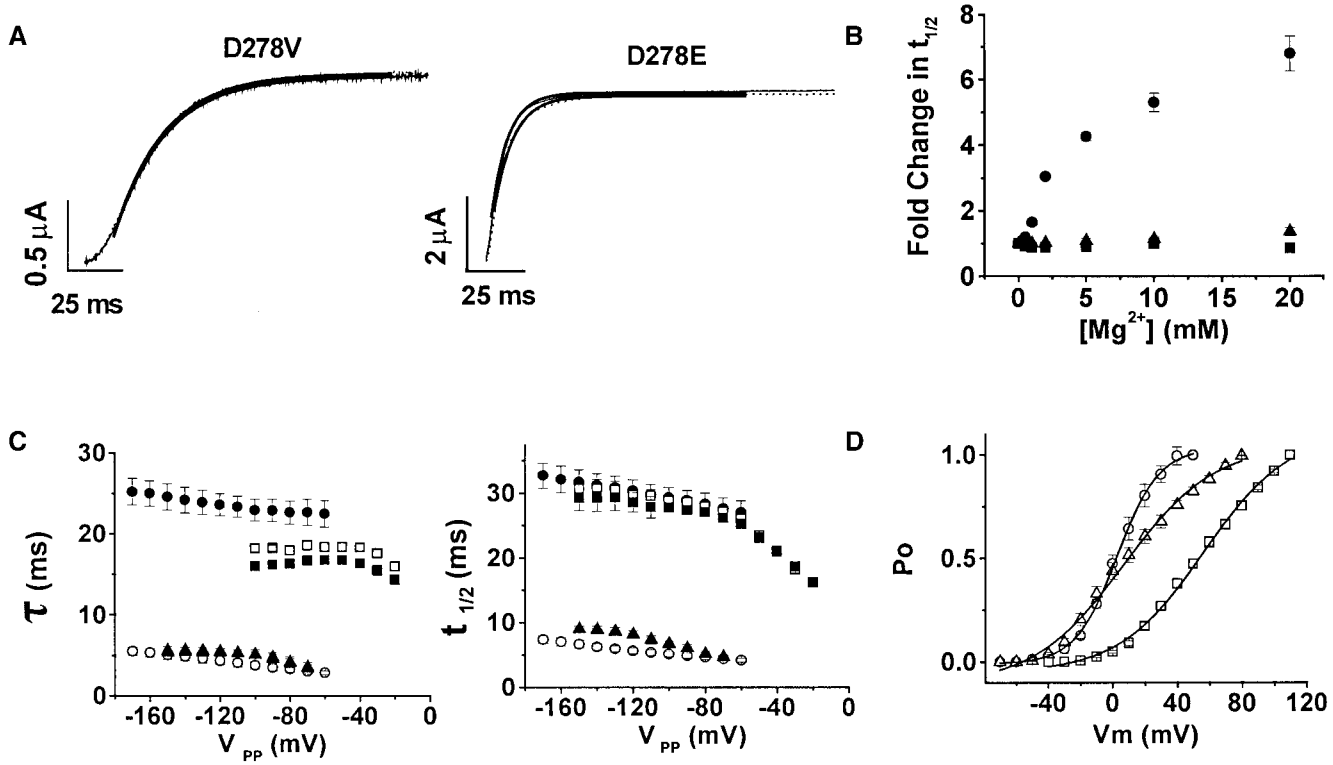

FIGURE 4. D278 mutants are insensitive to extracellular Mg^{2+}. (A) Representative current traces for D278V (left) and D278E (right) are shown. From a holding potential of −80 mV, test pulses to +60 mV were applied in the absence (solid lines) or presence (dashed lines) of 10 mM Mg^{2+}. Single exponential fits to the late rising phase are shown superimposed in bold on ionic current traces. (B) Values of $t_{1/2}$ at +60 mV for D278V (■), D278E (▲), and wild type (●) were measured in various concentrations of Mg^{2+} up to 20 mM, expressed as fold change in $t_{1/2}$, and plotted as a function of Mg^{2+} concentration. Values are shown as mean ± SEM, n = 3–4. (C) Values of τ (left) and $t_{1/2}$ (right) for D278V (■, □), D278E (▲, △), and wild type (●, ○) were measured as a function of prepulse potential in the presence (filled symbols) or absence (open symbols) of 10 mM Mg^{2+}. For the mutants, currents were evoked by a test pulse to +60 mV after 250 ms hyperpolarizing prepulses to the indicated potentials. Data for wild-type eag are the same as in Fig. 3 B. Values are shown as mean ± SEM, n = 3–5. (D) The probability of opening as a function of voltage for wild type (○), D278V (□), and D278E (△) channels was determined from isochronal tail currents in the absence of Mg^{2+}. Values are shown as mean ± SEM, n = 4–5. Po–V curves did not differ significantly in the presence of 10 mM Mg^{2+} (data not shown).

by screening the charge at D327. The results support the conclusion that D327, like D278, contributes to the Mg^{2+}-binding site by coordinating the ion.

Activation kinetics of the conservative mutant, D327E, were sensitive to extracellular Mg^{2+} (data not shown), in contrast to the results obtained with D278E (Fig. 4). Values for τ and $t_{1/2}$ measured either in the presence or absence of Mg^{2+} resembled those of the wild-type channel (data not shown). Mg^{2+} sensitivity of D327E suggests that the ion-binding site may be less sterically constrained near D327 than near D278.

D274 Is Not Required for Mg^{2+} Sensitivity, but Lies Near the Binding Site

D274 in S2 corresponds to an acidic residue that is widely conserved among voltage-dependent K^+ channels (Chandy and Gutman, 1995; Warmke and Ganetzky, 1994) (Fig. 1 B). In the Shaker K^+ channel, the D274 homologue is E283. Previous results strongly suggest that E283 lies near the extracellular surface of the Shaker protein, probably in a water-filled pocket or cavity (Tiwari-Woodruff et al., 2000). Upon Shaker activation, two S4 residues, R368 and R371, move into the vicinity of E283 (Tiwari-Woodruff et al., 2000). If S2 adopts an α-helical conformation, as suggested by perturbation analysis of Shaker and Kv2.1 K^+ channels (Monks et al., 1999; Hong and Miller, 2000; Li-Smerin et al., 2000a), in eag D274 and D278 will reside on the same face of the helix. In this case, D274 in eag may be located in a water-filled pocket that contains the Mg^{2+}-binding site. To test this hypothesis, we investigated whether D274 in S2 contributes to the Mg^{2+}-binding site in eag channels.

The mutations D274A and D274E were generated and expressed in *Xenopus* oocytes. In the absence of Mg^{2+}, the activation kinetics of D274A and D274E were similar to wild-type eag. And, as in wild-type, activation of D274A and D274E was significantly slowed by Mg^{2+}, indicating that D274 is not required for Mg^{2+} binding (Fig. 6 A). In fact, the neutralization mutation D274A

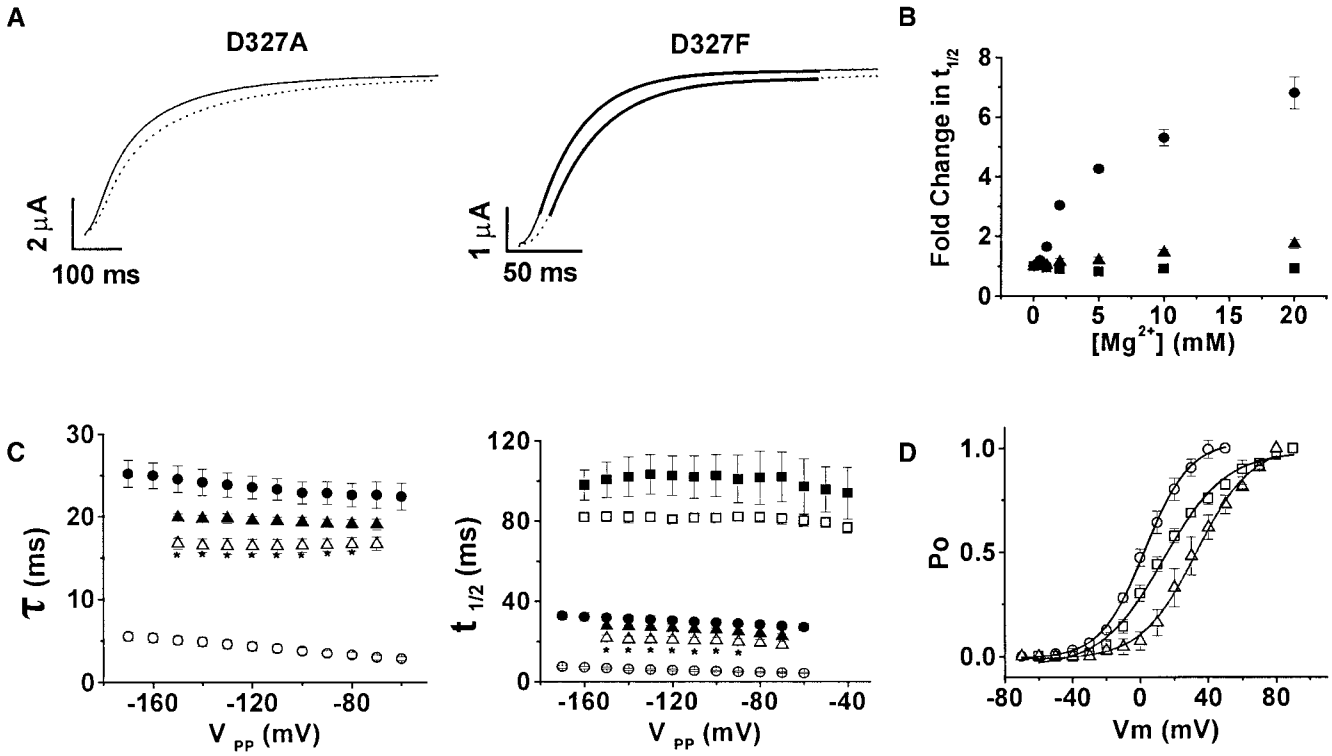

FIGURE 5. Mutations at D327 dramatically reduce sensitivity to Mg^{2+}. (A) Representative current traces for D327A (left) and D327F (right) are shown. From a holding potential of −80 mV, test pulses to +60 mV were applied in the absence (solid lines) or presence (dashed lines) of 10 mM Mg^{2+}. Single exponential fits to the late rising phase are shown superimposed in bold on D327F ionic current traces. (B) Values of $t_{1/2}$ at +60 mV for D327A (■), D327F (▲), and wild type (●) were measured in various concentrations of Mg^{2+} up to 20 mM, expressed as fold change in $t_{1/2}$, and plotted as a function of Mg^{2+} concentration. Values are shown as mean ± SEM, n = 3–4. (C) Values of τ (left) for D327F (▲, △) and wild type (●, ○), and values of $t_{1/2}$ (right) for D327A (■, □), D327F (▲, △), and wild type (●, ○) were measured as a function of prepulse potential in the presence (filled symbols) or absence (open symbols) of 10 mM Mg^{2+}. For the mutants, currents were evoked by a test pulse to +60 mV after 250 ms hyperpolarizing prepulses to the indicated potentials. Data for wild-type eag are the same as in Fig. 3 B. Values are shown as mean ± SEM, n = 3–5. For D327F, asterisks indicate τ and $t_{1/2}$ values that differed significantly in the presence and absence of Mg^{2+} (*, $P < 0.05$, ANOVA). (D) The probability of opening as a function of voltage for wild type (○), D327A (□), and D327F (△) channels was determined from isochronal tail currents in the absence of Mg^{2+}. Values are shown as mean ± SEM, n = 3–5. Po–V curves did not differ significantly in the presence of 10 mM Mg^{2+} (data not shown).

was as sensitive to Mg^{2+} as wild-type eag. Values of τ measured as a function of prepulse potential in the presence and absence of Mg^{2+} were similar in wild type and D274A (data not shown). In addition, the change in $t_{1/2}$ was virtually identical for Mg^{2+} concentrations up to 20 mM (Fig. 6 B). These results indicate that D274 does not contribute to eag's Mg^{2+}-binding affinity, and is therefore unlikely to interact with the bound ion.

Interestingly, two lines of evidence suggest that substituting D274 with the longer acidic amino acid, glutamate, increased the binding affinity for Mg^{2+}. First, Mg^{2+} had a larger effect on $t_{1/2}$ in D274E than in wild-type eag, with a shift in the dose response curve to lower Mg^{2+} concentrations (Fig. 6 B). Second, after removing Mg^{2+} from the bath solution, activation kinetics recovered more slowly in D274E than in wild-type eag (Fig. 6 C) or other Mg^{2+}-sensitive mutants such as D274A (data not shown). This effect was quantified by measuring the time interval between 10 and 90% of the peak current amplitude as a function of perfusion time during wash in and wash out of a bath solution containing 20 mM Mg^{2+} (Fig. 6 C). These results indicate that the mutation D274E decreases the Mg^{2+} dissociation rate, thereby increasing the apparent binding affinity. The data suggest that the longer glutamate residue is able to interact with the bound ion, unlike the original aspartate. We conclude that D274 is close to the binding site, consistent with the idea that D274 is exposed in the same water-filled pocket that contains the ion-binding site.

Hyperpolarizing Prepulses Reveal Mg^{2+}-sensitive Activation Kinetics in D284N

The position corresponding to D284 in eag is highly conserved among voltage gated K^+ channels (Fig. 1 B). In Shaker channels, the homologous residue E293 plays a key role in the mechanism of voltage-dependent activation. It contributes to the single channel gating charge, either by moving relative to the transmembrane electric field or by determining the profile of the

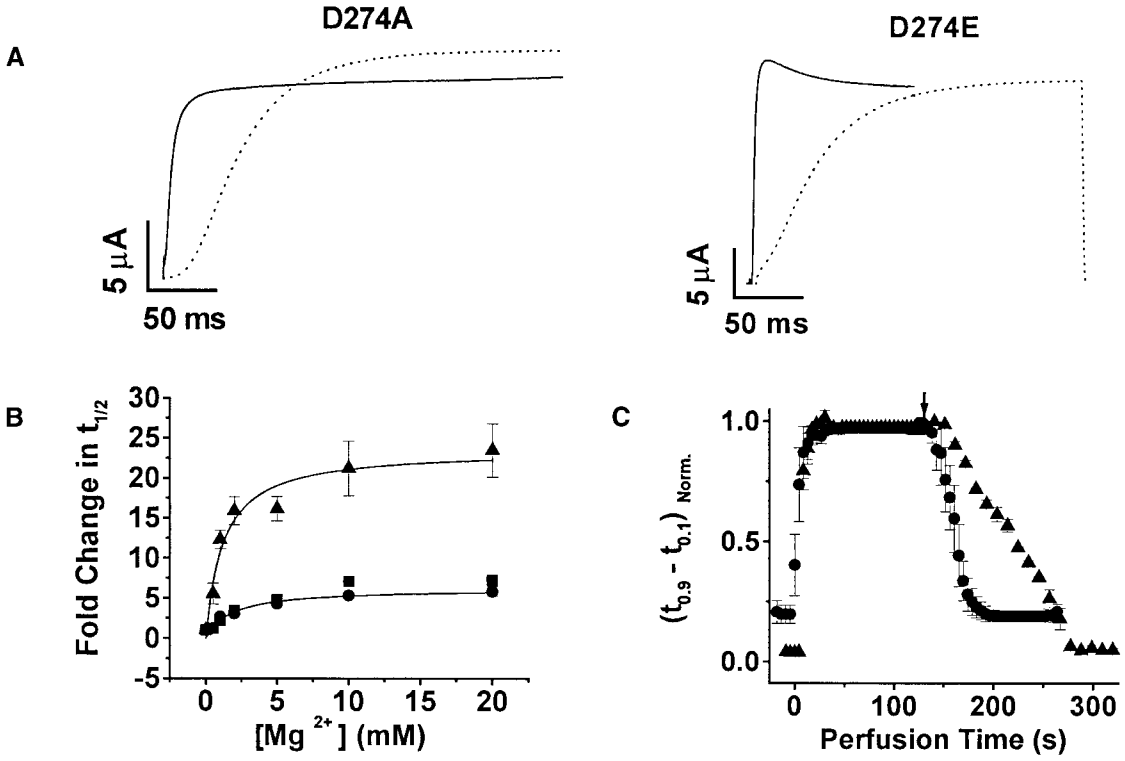

FIGURE 6. D274 mutants retain Mg^{2+} sensitivity. (A) Representative current traces for D274A (left) and D274E (right) are shown. From a holding potential of −80 mV, test pulses to +60 mV were applied in the absence (solid lines) or presence (dashed lines) of 10 mM Mg^{2+}. (B) Values of $t_{1/2}$ at +60 mV for D274A (■), D274E (▲), and wild type (●) were measured in various concentrations of Mg^{2+} up to 20 mM, expressed as fold change in $t_{1/2}$, and plotted as a function of Mg^{2+} concentration. Values are shown as mean ± SEM, n = 3–5. Half maximal Mg^{2+} concentrations, estimated by fitting rectangular hyperbolae (solid curves) to the data, were 3.5 mM for wild type and 1.2 mM for D274E. (C) Activation kinetics recover from Mg^{2+} more slowly in D274E channels than in wild-type eag. Cells expressing D274E and wild-type channels were subjected to continuous perfusion and held at −90 mV, with 400 ms test pulses to +60 mV applied at 4.5 s intervals during wash in for both wild type and D274E, and at 4.5 or 9.5 s intervals for wild type and D274E, respectively, during recovery. After establishing a baseline in the absence of Mg^{2+}, cells were perfused with extracellular solution containing 20 mM Mg^{2+} beginning at t = 0, followed by perfusion of the Mg^{2+}-free solution, beginning at the time indicated by the arrow. Activation kinetics were quantified by measuring the time interval between 10 and 90% of maximal current amplitude. This value was normalized to the longest interval (i.e., slowest kinetics), and plotted as a function of perfusion time. Values for wild type (●) and D274E (▲) are shown as mean ± SEM, n = 5.

field traversed by charge-moving residues in S4 (Seoh et al., 1996). In addition, this residue has been implicated in a structural interaction with a positively charged lysine in S4 (K374) in Shaker channels (Papazian et al., 1995; Tiwari-Woodruff et al., 1997).

In the eag mutants D284N and D284A, activation kinetics were fast, similar to wild-type eag, and unlike neutralization mutations at D278 and D327 (Fig. 7; compare to Figs. 4 and 5). Mg^{2+} had little effect on activation kinetics in D284N and D284A when currents were evoked by depolarizing from a holding potential of −80 mV (data not shown). However, hyperpolarizing prepulses revealed altered kinetics in the presence of Mg^{2+} in D284N (Fig. 7, A and B). A similar trend was evident in D284A channels (Fig. 7, A and C). These results indicate that activation kinetics in D284 mutants remain sensitive to hyperpolarizing prepulses, and that transitions occurring at hyperpolarized voltages retain their sensitivity to Mg^{2+}. Therefore, D284 is not required for Mg^{2+} binding.

Interestingly, the results indicate that the sensitivity of activation kinetics to prepulse voltages has been shifted to more hyperpolarized potentials in the D284 mutants, despite the fact that their Po–V curves were shifted in the depolarized direction (Fig. 7 D). The data suggest that mutations at D284 separate the voltage dependence of transitions in the eag activation pathway, shifting rate-determining, Mg^{2+}-sensitive transitions in the hyperpolarized direction, and channel opening in the depolarized direction. In the presence of Mg^{2+}, these transitions appeared to be faster in the mutants than in wild type (compare Figs. 2 and 7). This may explain the observation that ionic current kinetics in D284N and D284A were unaffected by Mg^{2+} at voltages where these channels opened. In wild type, in contrast, activation kinetics measured in the presence and

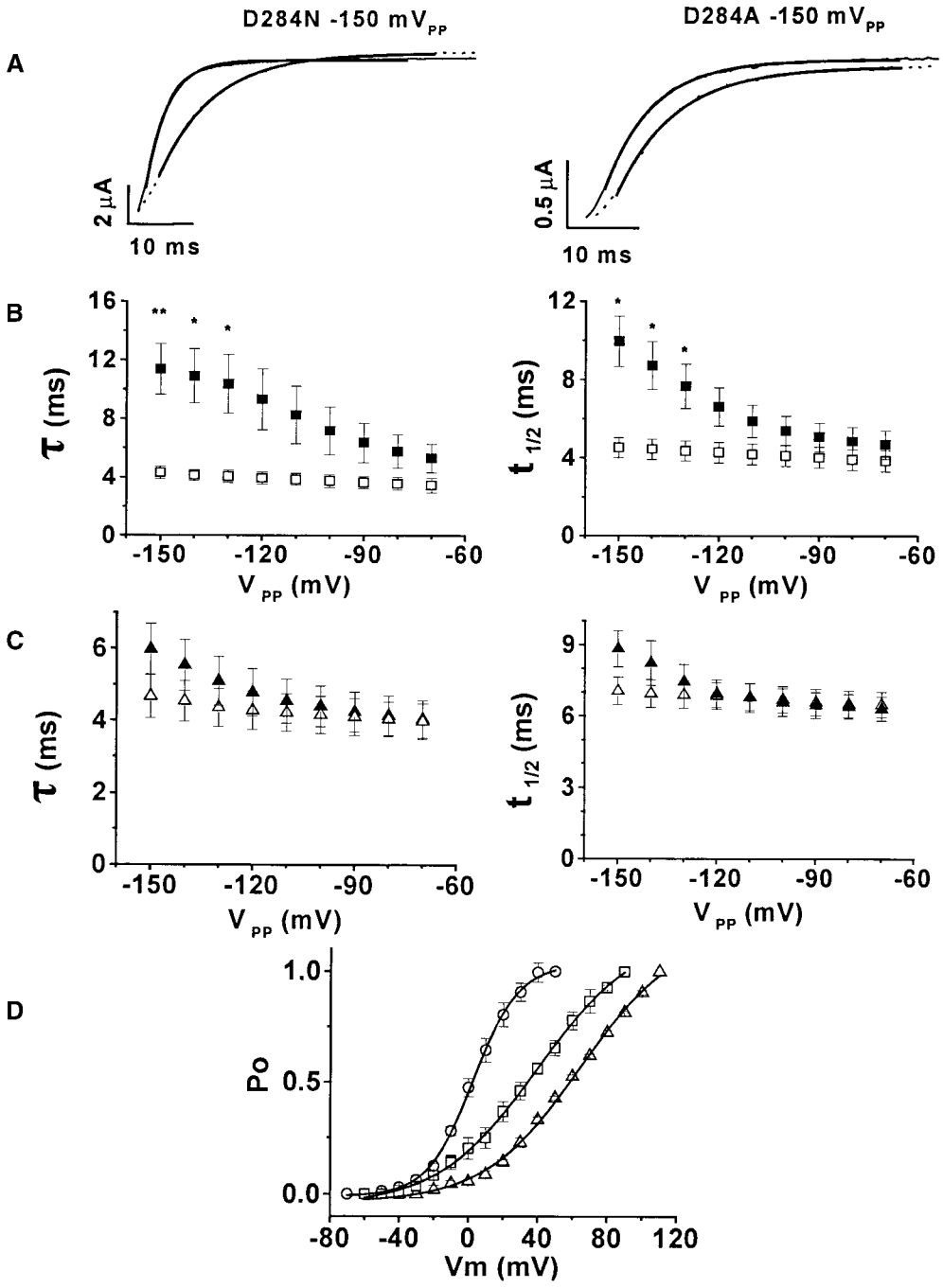

FIGURE 7. Hyperpolarizing prepulses reveal Mg^{2+}-sensitive transitions in D284 mutants. (A) Representative traces for D284N (left) and D284A (right) are shown. From a holding potential of −80 mV and in the absence (solid lines) or presence (dashed lines) of 10 mM Mg^{2+}, 250 ms prepulses to −150 mV were applied, followed by test pulses to +60 mV. Single exponential fits to the late rising phase are shown superimposed in bold on ionic current traces. (B) Values of τ (left) and $t_{1/2}$ (right) for D284N were measured as a function of prepulse potential in the presence (filled squares) or absence (open squares) of 10 mM Mg^{2+}. Currents were evoked by a test pulse to +60 mV after 250 ms hyperpolarizing prepulses to the indicated potentials. Values are shown as mean ± SEM, n = 5. For D284N, asterisks indicate τ and $t_{1/2}$ values that differed significantly in the presence and absence of Mg^{2+} (*, $P < 0.05$; **, $P < 0.01$; ANOVA). (C) Values of τ (left) and $t_{1/2}$ (right) for D284A were measured as a function of prepulse potential in the presence (▲) or absence (△) of 10 mM Mg^{2+}. Currents were evoked by a test pulse to +60 mV after 250 ms hyperpolarizing prepulses to the indicated potentials. Values are shown as mean ± SEM, n = 5. (D) The probability of opening as a function of voltage for wild type (○), D284N (□), and D284A (△) channels was determined from isochronal tail currents in the absence of Mg^{2+}. Values are shown as mean ± SEM, n = 3–4. Po–V curves did not differ significantly in the presence of 10 mM Mg^{2+} (data not shown).

absence of Mg^{2+} did not converge even at +100 mV (see Fig. 2). These results are consistent with the idea that D284 makes an important contribution to the gating mechanism, as does its homologue, E293, in Shaker channels (Seoh et al., 1996).

D319N Is Insensitive to Extracellular Mg^{2+}

D319, a residue near the intracellular end of S3, is highly conserved in different types of voltage-gated K^+ channels (Fig. 1 B). In Shaker, the analogous residue, D316, has been implicated in structural interactions

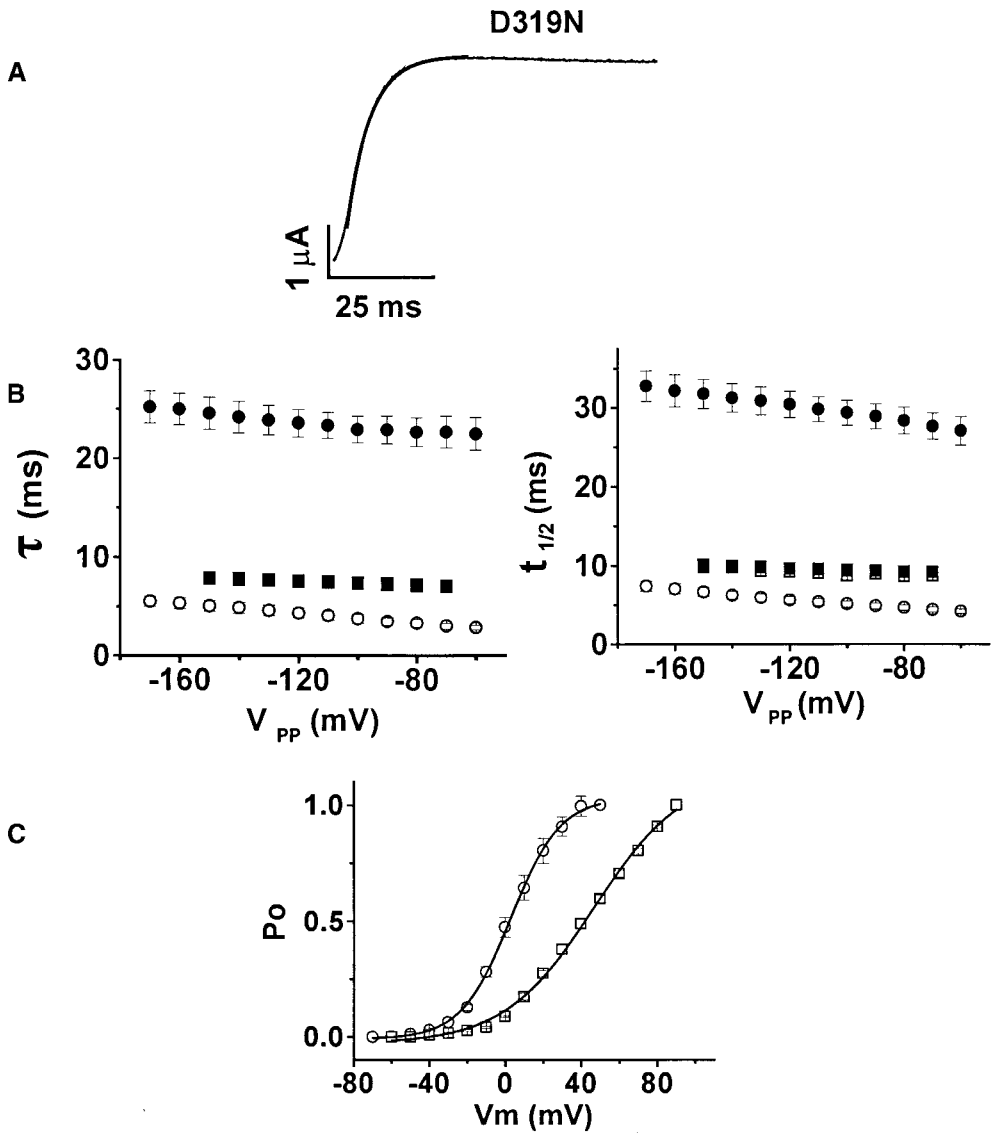

FIGURE 8. D319N is insensitive to extracellular Mg^{2+}. (A) Representative current traces for D319N are shown. From a holding potential of −80 mV, test pulses to +60 mV were applied in the absence (solid lines) or presence (dashed lines) of 10 mM Mg^{2+}. Single exponential fits to the late rising phase are shown superimposed in bold on ionic current traces. (B) Values of τ (left) and $t_{1/2}$ (right) for D319N (■, □) and wild type (●, ○) were measured as a function of prepulse potential in the presence (■, ●) or absence (○, □) of 10 mM Mg^{2+}. For D319N, currents were evoked by a test pulse to +60 mV after 250 ms hyperpolarizing prepulses to the indicated potentials. Data for wild-type eag are the same as in Fig. 3 B. Values are shown as mean ± SEM, n = 3–5. (C) The probability of opening as a function of voltage for wild type (○) and D319N (□) was determined from isochronal tail currents in the absence of Mg^{2+}. Values are shown as mean ± SEM, n = 3–5. Po–V curves did not differ significantly in the presence of 10 mM Mg^{2+} (data not shown).

with K374 in S4 that are essential for proper folding of the voltage sensor (Papazian et al., 1995; Tiwari-Woodruff et al., 1997).

In the eag mutant, D319N, ionic current kinetics were fast, similar to those of D284 neutralization mutants and wild-type eag in the absence of Mg^{2+} (Fig. 8 A; compare to Figs. 2 and 7). Mg^{2+} had no significant effect on the rate of activation of ionic currents evoked by depolarizing from −80 mV or after hyperpolarizing prepulses (Fig. 8, A and B). An extended range of prepulses was used because the D319 mutation shifted the Po–V curve in the depolarized direction (Fig. 8 C). In contrast to the wild-type channel, a transition to slower activation kinetics was not detected after hyperpolarized prepulses (Fig. 8 B).

The properties of D319N resemble those of D284N and D284A, except that hyperpolarizing prepulses did not reveal Mg^{2+}-sensitive, rate-limiting transitions. Significantly, mutations that neutralized either D284 or D319 resulted in fast kinetics that did not mimic the Mg^{2+}-bound state of wild-type eag, in contrast to neutralization mutations of D278 and D327. These results strongly suggest that D284 and D319 do not mediate the slowing of activation caused by Mg^{2+} binding. One possibility is that D319N, like D284N and D284A, primarily affects the eag gating pathway, and shifts the Mg^{2+}-sensitive, slow transitions in the hyperpolarized direction. If so, the shift would be greater in D319N than in D284N or D284A. Because D319N was Mg^{2+} insensitive in the experimentally accessible voltage range, however, we cannot rule out the possibility that D319 is required for Mg^{2+} binding.

DISCUSSION

Mg^{2+}-binding Site between S2 and S3

Extracellular Mg^{2+} dramatically slows voltage-dependent activation in eag K^+ channels (Terlau et al., 1996;

Schönherr et al., 1999; Tang et al., 2000). We have tested the hypothesis that eag-specific acidic residues found in transmembrane segments S2 and S3 contribute to the ion-binding site. Our results indicate that Mg^{2+} binds between S2 and S3 in the eag voltage sensor and thereby modulates voltage dependent activation. Eag-specific residues D278 in S2 and D327 in S3 are likely to coordinate the ion. In contrast, D284, an acidic residue in S2 that is conserved among all families of voltage-dependent K^+ channels, is not required for ion binding. Mutations at this position significantly altered the voltage dependence of transitions in the eag activation pathway, suggesting a role for S2 in channel gating. Neutralization of D319, a widely conserved acidic residue in S3, also affects gating or ion binding, or both. Interestingly, the data indicate that D274 in S2, another widely conserved acidic residue, is not required for ion binding, but is in the vicinity of the binding site. Identification of the Mg^{2+}-binding site in eag constrains the packing arrangement of transmembrane segments in the voltage sensor and provides insight into the molecular mechanism of Mg^{2+} action.

Several lines of evidence support the conclusion that D278 and D327 coordinate the Mg^{2+} ion. Neutralization mutations at these positions eliminated or significantly reduced Mg^{2+} modulation of activation kinetics. Importantly, neutralization of either D278 or D327 dramatically slowed activation, mimicking the kinetics of the Mg^{2+}-bound state of wild-type eag. The data suggest that Mg^{2+} slows activation in the wild-type channel by screening these negatively charged residues. The conclusion that D278 and D327 bind the ion is further strengthened by evidence that D274 in S2, one α-helical rung above D278, is unlikely to coordinate Mg^{2+}, but is quite close to the binding site. The mutation D274E increased the apparent affinity for Mg^{2+}, suggesting that glutamate, which has an acidic side chain ~1.5 Å longer than that of the original aspartate residue, is able to interact with an ion in the site.

The role of eag-specific residues in forming the binding site explains why modulation of activation kinetics by Mg^{2+} is unique to the eag family. Neutralizing either eag-specific aspartate residue eliminated Mg^{2+} sensitivity. It is worth noting that we have previously shown that a short sequence of primarily acidic residues in the S3–S4 loop is not required for Mg^{2+} binding, consistent with the presence of negatively charged residues at the end of S3 in a variety of K^+ channels (Tang et al., 2000). Our results can also account for the finding that some members of the eag family, such as elk, are insensitive to Mg^{2+} (Trudeau et al., 1999). Elk contains a glutamate residue at the position equivalent to D278 (Fig. 1 B) (Warmke and Ganetzky, 1994; Trudeau et al., 1999). We found that the D278E mutation abolished Mg^{2+} sensitivity of *Drosophila* eag, presumably due to steric constraints that prevent ion binding.

In the structures of various Mg^{2+}-binding sites, four, six, or eight ligands coordinate the ion (da Silva and Williams, 1991; Williams, 1993). The carboxylate side chains of D278 and D327 could provide at most four oxygen atoms to coordinate the bound Mg^{2+}. If these are the only ligands contributed by the eag protein, up to four water molecules ions may remain associated with the bound ion, depending on the geometry of the site. Other water molecules from the hydration shell are presumably lost upon binding.

Interestingly, a variety of cations slow activation in eag (Terlau et al., 1996). Given their qualitatively similar effects on ionic current kinetics, it is reasonable to propose that these different ions bind to the same site as Mg^{2+}. The extent to which an ion slows activation is correlated with its enthalpy of hydration (Terlau et al., 1996), consistent with our results, which suggest that an ion undergoes partial dehydration upon binding to eag. Presumably, the binding site must have some structural flexibility if it is able to accommodate different ions. Our results suggest the Mg^{2+}-binding site is sterically constrained near D278, but may be more flexible near D327. This may contribute to the ability of the site to bind a variety of ions.

Packing Arrangement of Transmembrane Segments in the Voltage Sensor

Residues that coordinate the same Mg^{2+} ion must be within atomic distance of one another. Therefore, our results suggest an important structural constraint for the packing arrangement of transmembrane segments in the eag voltage sensor. In a variety of high resolution protein structures containing bound Mg^{2+} ions, the center-to-center distance between Mg^{2+} and coordinating oxygen atoms is approximately 2.2 Å (Kankare et al., 1996; Andersson et al., 1997; Harutyunyan et al., 1997; Larsen et al., 1997; Sliz et al., 1997; Stec et al., 1998; Goldgur et al., 1999; Nichols et al., 1999). In these structures, the carboxylate groups of acidic residues that coordinate Mg^{2+} are within 2.7 to 4.3 Å of each other, providing an estimate of the likely distance between D278 in S2 and D327 in S3 when Mg^{2+} is bound.

Structural proximity between D278 and D327 is compatible with previously inferred structural constraints between S2, S3, and S4 in the Shaker voltage sensor (Papazian et al., 1995; Tiwari-Woodruff et al., 1997, 2000). Assuming structural conservation between Shaker and eag, we have combined our results from these channels to derive a model for the packing arrangement of segments S2, S3, and S4 in voltage-dependent K^+ channels (Fig. 9) (Papazian et al., 1995; Tiwari-Woodruff et al., 1997, 2000). This model repre-

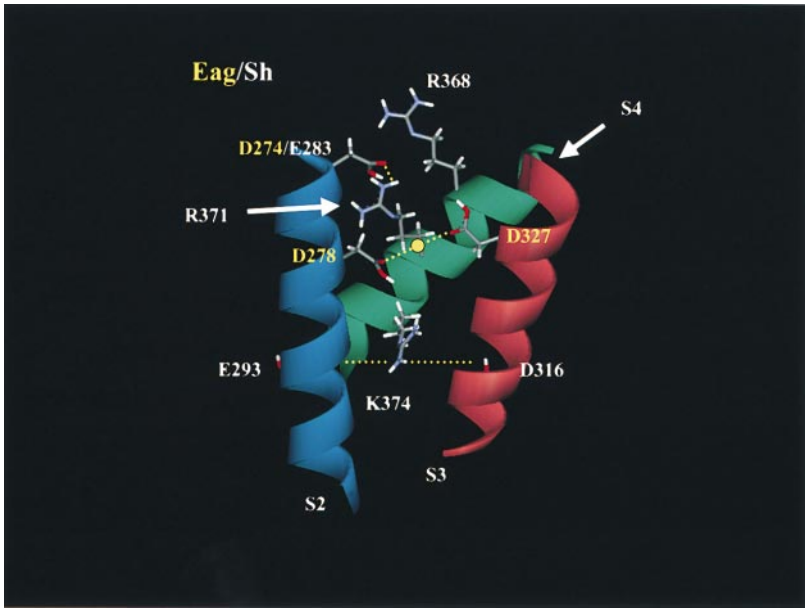

FIGURE 9. Model for the packing arrangement of transmembrane segments S2 (blue), S3 (red), and S4 (green) in the voltage sensor of K^+ channels. The model contains structural constraints (dotted lines) inferred from characterization of the Mg^{2+}-binding site in eag (this study) and from second site suppressor analysis of Shaker (Papazian et al., 1995; Tiwari-Woodruff et al., 1997). The transmembrane segments are shown in α-helical conformation with fully extended side chains. A yellow circle denotes a bound Mg^{2+} ion in eag. Side chains of pertinent residues have been labeled according to Shaker (white) and, in some cases, eag (yellow) numbering. Side chains of other residues are not shown. According to analysis of Shaker channels, the pictured conformation would represent the activated conformation of the voltage sensor (Tiwari-Woodruff et al., 2000). The model was generated using the programs InsightII and WebLab Viewer Lite (Molecular Simulations).

sents the activated conformation of the voltage sensor, in which E283 in S2 (the Shaker homologue of D274) achieves its closest proximity with R371, the fourth basic residue in the Shaker S4 segment (Tiwari-Woodruff et al., 2000). Importantly, the eag results have been used to constrain the relative positions of segments S2 and S3, which cannot be determined from the Shaker results alone (Tiwari-Woodruff et al., 1997). We have assumed that S2, S3, and S4 are α-helical, consistent with the results of perturbation analysis in Shaker and Kv2.1 channels (Monks et al., 1999; Hong and Miller, 2000; Li-Smerin et al., 2000a).

In Fig. 9, the S4 segment is shown tilted relative to S2 and S3, a feature introduced in our earlier model to satisfy the structural constraints inferred for Shaker (Tiwari-Woodruff et al., 1997). Interestingly, Li-Smerin et al. (2000b) have recently reported the results of perturbation analysis on the putative outer surface of the Shaker pore domain. Their data suggest that the voltage sensor packs against the pore via a localized interaction surface. Significantly, this surface is tilted relative to the center axis of the pore at an angle very similar to that of the S4 segment in our model (Tiwari-Woodruff et al., 1997). Thus, results from three independent approaches, second site suppressor analysis in Shaker (Papazian et al., 1995; Tiwari-Woodruff et al., 1997, 2000), characterization of the Mg^{2+}-binding site in eag (this study), and perturbation analysis of the pore domain in Shaker (Li-Smerin et al., 2000b) support the packing model for the voltage sensor proposed in Fig. 9.

Results obtained with both Shaker and eag strongly suggest that there is an externally facing, water-filled pocket next to S2. In eag, extracellular Mg^{2+} is able to access a site formed by D278 in S2 and D327 in S3, which would project into the pocket to coordinate the ion. In an α-helix, D274 in S2, located one rung above D278, would also be exposed in the same cavity. Significantly, previous work in Shaker channels indicates that E283, the S2 residue analogous to D274 in eag, is located in a cavity near the extracellular surface of the protein (Tiwari-Woodruff et al., 2000). Upon activation of Shaker channels, two S4 residues, first R368 and then R371, move into the vicinity of E283 (Tiwari-Woodruff et al., 2000). Taken together, the eag and Shaker results suggest that voltage-dependent K^+ channels contain a water-filled pocket lined by S2 and S3. S4 residues also project into this space, at least in the activated conformation. An important difference between the pockets in Shaker and eag channels determines their differential sensitivity to extracellular Mg^{2+}. In eag, acidic residues contribute to a Mg^{2+}-binding site at the bottom of the cavity. In Shaker, in contrast, the cavity may be shallower than in eag due to the presence of hydrophobic residues at the positions analogous to D278 and D327 (Fig. 1 B). We conclude that voltage-dependent K^+ channels contain an externally facing, water-filled pocket between S2, S3, and S4.

Interestingly, this pocket may be nearly isopotential with the extracellular solution. In Shaker, a cysteine substituted for E283 in S2 shows very similar reactivity at depolarized and hyperpolarized potentials (Tiwari-Woodruff et al., 2000). In eag, Mg^{2+} affects activation kinetics at +100 mV (Fig. 2), indicating that Mg^{2+} is not expelled from its binding site by depolarizing the cell.

Possible Mechanism of Mg^{2+} Action

Results obtained in a variety of laboratories suggest that activation of K^+ channels involves at least two voltage-

dependent conformational changes per subunit (Bezanilla et al., 1994; Perozo et al., 1994; Sigg et al., 1994; Stefani et al., 1994; Zagotta et al., 1994a,b; Cha and Bezanilla, 1997; Baker et al., 1998; Schoppa and Sigworth, 1998a,b). Both S2 and S4 are likely to participate in conformational changes during the first phase of activation, which occurs at hyperpolarized potentials (Cha and Bezanilla, 1997; Baker et al., 1998). Evidence for involvement of S2 in this phase includes site-directed fluorescent measurements in Shaker (Cha and Bezanilla, 1997) and functional analysis of eag mutants (this study). Involvement of the S4 segment in the first phase is likely because intermediate conformations of S4, which do not correspond to either the fully resting or the fully activated conformation, have been detected (Baker et al., 1998; Tiwari-Woodruff et al., 2000). The second phase of activation occurs at more depolarized potentials than the first, involves an additional movement of S4, and is closely correlated with channel opening (Bezanilla et al., 1994; Sigg et al., 1994; Stefani et al., 1994; Zagotta et al., 1994a,b; Mannuzzu et al., 1996; Cha and Bezanilla, 1997; Baker et al., 1998). In Shaker, R371 in S4 moves into proximity with E283 in S2 during the second phase of the mechanism (Tiwari-Woodruff et al., 2000). Although this picture of activation is undoubtedly oversimplified, it provides a compatible synthesis of results obtained using several approaches.

Based on this picture of activation, we propose a speculative model of the mechanism by which Mg^{2+} modulates voltage-dependent gating in eag. We previously suggested that Mg^{2+} modulates two different voltage-dependent transitions during eag activation, corresponding to the two phases described above (Tang et al., 2000). We have now located the Mg^{2+}-binding site within the water-filled pocket between S2 and S3, an ideal location for modulating the kinetics of both phases of activation. Mg^{2+} could modulate the kinetics of the first phase of activation by forming a bridge between S2 and S3, and thereby slowing conformational changes of S2 relative to S3. During both phases of activation, bound Mg^{2+} could slow the rate at which positively charged S4 residues (the eag homologues of R368 and R371 in Shaker) move into the pocket to interact with D274. Although this model is speculative, it is compatible with the emerging picture of the physical mechanism of voltage-dependent gating in K^+ channels and with our previous characterization of Mg^{2+} action on ionic and gating currents in eag.

Our results are consistent with the expectation that the overall structure and function of the voltage sensor is conserved in K^+ channels that have a wide range of kinetics and differential regulation. Presumably, the detailed kinetic properties of activation in individual types of K^+ channels are conferred by sequence differences that result in subtle structural changes despite a conserved architecture.

We are grateful to Dr. James Bowie for helpful discussions and to members of the Papazian lab for their comments on the manuscript.

This work was supported by grants to D.M. Papazian from the National Institutes of Health (NIH; GM43459); the American Heart Association, Western States Affiliate; and the Laubisch fund for cardiovascular research at UCLA. W.R. Silverman was partially supported by an NIH predoctoral training grant (GM08496).

Submitted:24 August 2000
Revised: 2 October 2000
Accepted:2 October 2000

REFERENCES

Aggarwal, S.K., and R. MacKinnon. 1996. Contribution of the S4 segment to gating charge in the Shaker K^+ channel. *Neuron.* 16: 1169–1177.

Andersson, M., A. Malmendal, S. Linse, I. Iversson, S. Forsen, and L.A. Svensson. 1997. Structural basis for the negative allostery between Ca^{2+} and Mg^{2+} binding in the intracellular Ca^{2+} receptor calbindin D9k. *Protein Sci.* 6:1139–1147.

Baker, O.S., H.P. Larsson, L.M. Mannuzzu, and E.Y. Isacoff. 1998. Three transmembrane conformations and sequence-dependent displacement of the S4 domain in Shaker K^+ channel gating. *Neuron.* 20:1283–1294.

Bezanilla, F., and C.M. Armstrong. 1977. Inactivation of the sodium channel. I. Sodium current experiments. *J. Gen. Physiol.* 70:549–566.

Bezanilla, F., E. Perozo, and E. Stefani. 1994. Gating of Shaker K^+ channels: II. The components of gating currents and a model of channel activation. *Biophys. J.* 66:1011–1021.

Brüggemann, A., L.A. Pardo, W. Stuhmer, and O. Pongs. 1993. Ether-à-go-go encodes a voltage-gated channel permeable to K^+ and Ca^{2+} and modulated by cAMP. *Nature.* 365:445–448.

Cha, A., and F. Bezanilla. 1997. Characterizing voltage-dependent conformational changes in the Shaker K^+ channel with fluorescence. *Neuron.* 19:1127–1140.

Cha, A., G.E. Snyder, P.R. Selvin, and F. Bezanilla. 1999. Atomic scale movement of the voltage-sensing region in a potassium channel measured via spectroscopy. *Nature.* 402:809–813.

Chandy, K.G., and G.A. Gutman. 1995. Voltage-gated potassium channel genes. *In* Ligand- and Voltage-Gated Ion Channels. R.A. North, editor. CRC Press, Boca Raton, Fl. 1–71.

Cole, K.S., and Moore, J.W. 1960. Potassium ion current in the squid giant axon: dynamic characteristic. *Biophys. J.* 1:1–14.

da Silva, J.J.R.F., and R.J.P. Williams. 1991. The Biological Chemistry of the Elements: The Inorganic Chemistry of Life. Oxford University Press, New York. 561 pp.

Dougherty, D.A. 1996. Cation-π interactions in chemistry and biology: a new view of benzene, Phe, Tyr, and Trp. *Science.* 271:163–168.

Frings, S., N. Brüll, C. Dzeja, A. Angele, V. Hagen, U.B. Kaupp, and A. Baumann. 1998. Characterization of ether-à-go-go channels present in photoreceptors reveals similarity to I_{Kx}, a K^+ current in rod inner segments. *J. Gen. Physiol.* 111:583–599.

Ganetzky, B., G.A. Robertson, G.F. Wilson, M.C. Trudeau, and S.A. Titus. 1999. The eag family of K^+ channels in *Drosophila* and mammals. *Annu. NY Acad. Sci.* 868:356–369.

Glauner, K.S., L.M. Mannuzzu, C.S. Gandhi, and E.Y. Isacoff. 1999. Spectroscopic mapping of voltage sensor movement in the Shaker potassium channel. *Nature.* 402:813–817.

Goldgur, Y., G.H. Cohen, T. Fugiwara, T. Yoshinaga, T. Fuishita, H. Sugimoto, T. Endo, H. Murai., and D.R. Davies. 1999. Structure of the HIV-1 integrase catalytic domain complexed with an inhibitor: a platform for antiviral drug design. *Proc. Natl. Acad. Sci. USA*. 96:13040–13043.

Harutyunyan E.H., V.Y. Oganessyan, N.N. Oganessyan, S.M. Avaeva, T.I. Nazarova, N.N. Vorobyeva, S.A. Kurilova, R. Huber, T. Mather. 1997. Crystal structure of holo inorganic pyrophosphatase from *Escherichia coli* at 1.9 Å resolution. Mechanism of hydrolysis. *Biochemistry*. 36:7754–7760.

Hong, K.H., and C. Miller. 2000. The lipid-protein interface of a Shaker K^+ channel. *J. Gen. Physiol.* 115:51–58.

Hoshi, T., W.N. Zagotta, and R.W. Aldrich. 1994. Shaker potassium channel gating. I: Transitions near the open state. *J. Gen. Physiol.* 103:249–278.

Kankare, J., T. Salminen, R. Lahti, B.S. Cooperman, A.A. Baykov, and A. Goldman. 1996. Crystallographic identification of metal binding sites in *Escherichia coli* inorganic pyrophosphatase. *Biochemistry*. 35:4770–4777.

Landt, O., H.P. Grunert, and U. Hahn. 1990. A general method for rapid site-directed mutagenesis using the polymerase chain reaction. *Gene*. 96:125–128.

Larsen, T.M., M.M. Benning, G.E. Wesenberg, I. Rayment, and G.H. Reed. 1997. Ligand-induced domain movement in pyruvate kinase: structure of the enzyme from rabbit muscle with Mg^{2+}, K^+, and L-phospholactate at 2.7Å resolution. *Arch. Biochem. Biophys.* 345:199–206.

Larsson, H.P., O.S. Baker, D.S. Dhillon, and E.Y. Isacoff. 1996. Transmembrane movement of the Shaker K^+ channel S4. *Neuron*. 16:387–397.

Ledwell, J.L., and R.W. Aldrich. 1999. Mutations in the S4 region isolate the final voltage-dependent cooperative step in potassium channel activation. *J. Gen. Physiol.* 113:389–414.

Li-Smerin, Y., D.H. Hackos, and K.J. Swartz. 2000a. α-helical structural elements within the voltage-sensing domains of a K^+ channel. *J. Gen. Physiol.* 115:33–50.

Li-Smerin, Y., D.H. Hackos, and K.J. Swartz. 2000b. A localized interaction surface for voltage-sensing domains on the pore domain of a K^+ channel. *Neuron*. 25:411–423.

Liman, E.R., P. Hess, F. Weaver, and G. Koren. 1991. Voltage-sensing residues in the S4 region of a mammalian K^+ channel. *Nature*. 353:752–756.

Ludwig, J., H. Terlau, F. Wunder, A. Brüggemann, L.A. Pardo, A. Marquardt, W. Stuhmer, and O. Pongs. 1994. Functional expression of a rat homologue of the voltage gated ether-à-go-go potassium channel reveals differences in selectivity and activation kinetics between the *Drosophila* channel and its mammalian counterpart. *EMBO (Eur. Mol. Biol. Organ.) J.* 13:4451–4458.

Mannuzzu, L.M., M.M. Moronne, and E.Y. Isacoff. 1996. Direct physical measure of conformational rearrangement underlying potassium channel gating. *Science*. 271:213–216.

Monks, S.A., D.J. Needleman, and C. Miller. 1999. Helical structure and packing orientation of the S2 segment in the Shaker K^+ channel. *J. Gen. Physiol.* 113:415–423.

Nichols, M.D., K.A. DeAngelis, J.L. Keck, and J.M. Berger. 1999. Structure and function of an archaeal topoisomerase VI subunit with homology to meiotic recombination factor Spo11. *EMBO (Eur. Mol. Biol. Organ.) J.* 18:6177–6188.

Papazian, D.M., L.C. Timpe, Y.N. Jan, and L.Y. Jan. 1991. Alteration of voltage-dependence of Shaker potassium channel by mutations in the S4 sequence. *Nature*. 349:305–310.

Papazian, D.M., X.M. Shao, S.A. Seoh, A.F. Mock, Y. Huang, and D.H. Wainstock. 1995. Electrostatic interactions of S4 voltage sensor in Shaker K^+ channel. *Neuron*. 14:1293–1301.

Perozo, E., L. Santacruz-Toloza, E. Stefani, F. Bezanilla, and D.M. Papazian. 1994. S4 mutations alter gating currents of Shaker K^+ channels. *Biophys. J.* 66:345–354.

Planells-Cases, R., A.V. Ferrer-Montiel, C.D. Patten, and M. Montal. 1995. Mutation of conserved negatively charged residues in the S2 and S3 transmembrane segments of a mammalian K^+ channel selectively modulates channel gating. *Proc. Natl. Acad. Sci. USA*. 92:9422–9426.

Sarkar, G., and S.S. Sommer. 1990. The "megaprimer" method of site-directed mutagenesis. *Biotechniques*. 8:404–407.

Schönherr, R., S. Hehl, H. Terlau, A. Baumann, and S.H. Heinemann. 1999. Individual subunits contribute independently to slow gating of bovine eag potassium channels. *J. Biol. Chem.* 274: 5362–5369.

Schoppa, N.E., and F.J. Sigworth. 1998a. Activation of Shaker potassium channels. I. Characterization of voltage-dependent transitions. *J. Gen. Physiol.* 111:271–294.

Schoppa, N.E., and F.J. Sigworth. 1998b. Activation of Shaker potassium channels. III. An activation gating model for wild-type and V2 mutant channels. *J. Gen. Physiol.* 111:313–342.

Seoh, S.A., D. Sigg, D.M. Papazian, and F. Bezanilla. 1996. Voltage-sensing residues in the S2 and S4 segments of the Shaker K^+ channel. *Neuron*. 16:1159–1167.

Shi, W., R.S. Wymore, H.S. Wang, Z. Pan, I.S. Cohen, D. McKinnon, and T.E. Dixon. 1997. Identification of two nervous system-specific members of the erg potassium channel family. *J. Neurosci*. 17: 9423–9432.

Sigg, D., E. Stefani, and F. Bezanilla. 1994. Gating current noise produced by elementary transitions in Shaker potassium channels. *Science*. 264:578–582.

Sliz, P., R. Engleman, W. Hengstenberg, and E.F. Pai. 1997. The structure of enzyme IIA lactose from *Lactococcus lactis* reveals a new fold and points to possible interactions of a multicomponent system. *Structure*. 5:775–788.

Smith-Maxwell, C.J., J.L. Ledwell, and R.W. Aldrich. 1998. Uncharged S4 residues and cooperativity in voltage-dependent potassium channel activation. *J. Gen. Physiol.* 111:421–439.

Starace, D.M., E. Stefani, and F. Bezanilla. 1997. Voltage-dependent proton transport by the voltage sensor of the Shaker K^+ channel. *Neuron*. 19:1319–1327.

Stec, B., M.J. Mehir, C. Brennan, M. Nolte, and E.R. Kantrowitz. 1998. Kinetic and X-ray structural studies of three mutant *E. coli* alkaline phosphatases: insights into the catalytic mechanism without the nucleophile Ser102. *J. Mol. Biol.* 227:647–662.

Stefani, E., L. Toro, E. Perozo, and F. Bezanilla. 1994. Gating of Shaker K^+ channels: I. Ionic and gating currents. *Biophys. J.* 66: 996–1010.

Tang, C.-Y., and D.M. Papazian. 1997. Transfer of voltage independence from a rat olfactory channel to the *Drosophila* ether-à-go-go K^+ channel. *J. Gen. Physiol.* 109:301–311.

Tang, C.-Y., F. Bezanilla, and D.M. Papazian. 2000. Extracellular Mg^{2+} modulates slow gating transitions and the opening of *Drosophila* ether-à-go-go potassium channels. *J. Gen Physiol.* 115:319–338.

Terlau, H., J. Ludwig, R. Steffan, O. Pongs, W. St¸hmer, and S.H. Heinemann. 1996. Extracellular Mg^{2+} regulates activation of rat eag potassium channel. *Pflugers Arch.* 432:301–312.

Timpe, L.C., T.L. Schwarz, B.L. Tempel, D.M. Papazian, Y.N. Jan, and L.Y. Jan. 1988. Expression of functional potassium channels from *Shaker* cDNA in *Xenopus* oocytes. *Nature*. 331:143–145.

Tiwari-Woodruff, S.K., C.T. Schulteis, A.F. Mock, and D.M. Papazian. 1997. Electrostatic interactions between transmembrane segments mediate folding of Shaker K^+ channel subunits. *Biophys. J.* 72:1489–1500.

Tiwari-Woodruff, S.K., M.A. Lin, C.T. Schulteis, and D.M. Papazian. 2000. Voltage-dependent structural interactions in the Shaker K^+

channel. *J. Gen. Physiol.* 115:123–138.

Trudeau, M.C., S.A. Titus, J.L. Branchaw, B. Ganetzky, and G.A. Robertson. 1999. Functional analysis of a mouse brain Elk-type K^+ channel. *J. Neurosci.* 19:2906–2918.

Warmke, J., R. Drysdale, and B. Ganetzky. 1991. A distinct potassium channel polypeptide encoded by the *Drosophila* eag locus. *Science.* 252:1560–1562.

Warmke, J.W., and B. Ganetzky. 1994. A family of potassium channel genes related to eag in *Drosophila* and mammals. *Proc. Natl. Acad. Sci. USA.* 91:3438–3442.

Wei, A., T. Jegla, and L. Salkoff. 1996. Eight potassium channel families revealed by the *C. elegans* genome project. *Neuropharmacology.* 35:805–829.

Williams, R.J.P. 1993. Magnesium: an introduction to its biochemistry. *In* Magnesium and the Cell. N.J. Birch, editor. Academic Press, New York. 15–29.

Williams, K., A.J. Pahk, K. Kashiwagi, T. Masuko, N.D. Nguyen, and K. Igarashi. 1998. The selectivity filter of the N-methyl-D-aspartate receptor: a tryptophan residue controls block and permeation of Mg^{2+}. *Mol. Pharmacol.* 53:933–941.

Wouters, J. 1998. Cation-π (Na^+-Trp) interactions in the crystal structure of tetragonal lysozyme. *Protein Sci.* 7:2472–2475.

Zagotta, W.N., T. Hoshi, J. Dittman, and R.W. Aldrich. 1994a. Shaker potassium channel gating. II: Transitions in the activation pathway. *J. Gen. Physiol.* 103:279–319.

Zagotta, W.N., T. Hoshi, and R.W. Aldrich. 1994b. Shaker potassium channel gating. III: Evaluation of kinetic models for activation. *J. Gen. Physiol.* 103:321–362.